

Article

# Microwave Dielectric Properties of $\beta$ -CaSiO<sub>3</sub> Glass–Ceramics Prepared Using Two-Step Heat Treatment

Jin-Seok Baek, Nak-Beom Jo and Eung-Soo Kim \* 

Department of Advanced Materials Engineering, Graduate School, Kyonggi University, Suwon 443-760, Korea; cosmoflip@kyonggi.ac.kr (J.-S.B.); pilot3705@kyonggi.ac.kr (N.-B.J.)

\* Correspondence: eskim@kyonggi.ac.kr; Tel.: +82-32-2499764

**Abstract:** The microwave dielectric properties of  $\beta$ -CaSiO<sub>3</sub> glass–ceramics are compared with those of  $\alpha$ -CaSiO<sub>3</sub> ceramics.  $\beta$ -CaSiO<sub>3</sub> is prepared using glass–ceramics method with two-step heat treatment at 730 °C for 1–7 h and at 900 °C for 3 h, and  $\alpha$ -CaSiO<sub>3</sub> is prepared using conventional solid-state reaction and sintered at 1460–1500 °C for 3 h. With increasing holding time at 730 °C, the degree of crystallisation and  $Q_f$  of the  $\beta$ -CaSiO<sub>3</sub> glass–ceramics increased. The  $\beta$ -CaSiO<sub>3</sub> specimens heat-treated at 730 °C for 3 h and 900 °C for 3 h exhibit the following dielectric properties:  $K = 6.57$ ,  $TCF = -36.22$  ppm/°C, and  $Q_f = 52,400$  GHz (highest) for the entire range of heat treatment conditions. The  $Q_f$  difference between  $\beta$ -CaSiO<sub>3</sub> and  $\alpha$ -CaSiO<sub>3</sub> could be explained by the bond characteristics using Rietveld refinement. FT-IR analysis shows that the Ca–O bond is the dominant factor for the  $Q_f$  of CaSiO<sub>3</sub> ceramics compared to the Si–O bond. The higher  $Q_f$  of  $\beta$ -CaSiO<sub>3</sub> than that of  $\alpha$ -CaSiO<sub>3</sub> can be attributed to the higher bond strength of Ca–O for  $\beta$ -CaSiO<sub>3</sub> than that for  $\alpha$ -CaSiO<sub>3</sub>.

**Keywords:**  $\beta$ -CaSiO<sub>3</sub>;  $\alpha$ -CaSiO<sub>3</sub>; glass–ceramics; microwave dielectric properties; rietveld refinement



**Citation:** Baek, J.-S.; Jo, N.-B.; Kim, E.-S. Microwave Dielectric Properties of  $\beta$ -CaSiO<sub>3</sub> Glass–Ceramics Prepared Using Two-Step Heat Treatment. *Processes* **2021**, *9*, 2180. <https://doi.org/10.3390/pr9122180>

Academic Editor: Sung-Churl Choi

Received: 8 November 2021

Accepted: 30 November 2021

Published: 3 December 2021

**Publisher's Note:** MDPI stays neutral with regard to jurisdictional claims in published maps and institutional affiliations.



**Copyright:** © 2021 by the authors. Licensee MDPI, Basel, Switzerland. This article is an open access article distributed under the terms and conditions of the Creative Commons Attribution (CC BY) license (<https://creativecommons.org/licenses/by/4.0/>).

## 1. Introduction

The fourth industrial revolution, which is the advancement of 5G telecommunication, Internet of Things (IoT), and automotive vehicles, typically requires high-frequency communication for integration and high performance of the future technologies. Low-temperature co-fired ceramics (LTCC) can be co-fired with conductive electrodes. Thus, LTCC dielectric materials can be incorporated into microwave devices for reducing their manufacturing cost [1,2]. However, for this incorporation, LTCC dielectric materials require several characteristics, such as a low dielectric constant ( $K$ ) of  $<10$  for high-speed data transmission and minimization of signal delay, a high quality factor ( $Q_f$ ) for prominent frequency selectivity, a small temperature coefficient of resonant frequency ( $TCF$ ) for thermal stability, and a low sintering temperature of  $<950$  °C for co-firing with conductive electrodes, such as silver and copper [3,4]. Glass–ceramics prepared using two-step heat treatment are promising as LTCC substrate materials [5], in which the first step involves homogeneous formation of nuclei, and the second step involves the crystal growth of the nuclei [6].

CaSiO<sub>3</sub> is a promising candidate for LTCC because of its low  $K$  and high  $Q_f$  at a fabrication temperature of  $<950$  °C. CaSiO<sub>3</sub> has two polymorphs, and it undergoes phase transition at 1125 °C [7].  $\beta$ -CaSiO<sub>3</sub> has SiO<sub>4</sub> tetrahedral chain structure and  $\alpha$ -CaSiO<sub>3</sub> has three-membered SiO<sub>4</sub> tetrahedral ring structure [8,9], and the dielectric properties of  $\beta$ -CaSiO<sub>3</sub> and  $\alpha$ -CaSiO<sub>3</sub> prepared using conventional solid-state reaction are obtained at 16,850 and 42,200 GHz, respectively [10,11]. However, the sintering temperatures for obtaining the LTCC dielectric materials are high, such as 1400 °C for  $\alpha$ -CaSiO<sub>3</sub> and 1100 °C for  $\beta$ -CaSiO<sub>3</sub>, and it is difficult to obtain dense  $\beta$ -CaSiO<sub>3</sub> using the conventional solid-state reaction.

According to Mohammadi et al. [12], the nucleation and crystallisation temperatures of  $\beta$ -CaSiO<sub>3</sub> glass are 730 and 860 °C, respectively. However, the microwave dielectric properties of  $\beta$ -CaSiO<sub>3</sub> glass–ceramics have not been reported.

If the structure of the glass and crystalline phase are similar, it is easier to generate the crystalline phase from the glass. In the case of CaSiO<sub>3</sub>, it has been reported that the structural characteristics of  $\alpha$ -CaSiO<sub>3</sub> and  $\beta$ -CaSiO<sub>3</sub> are [Si<sub>3</sub>O<sub>9</sub>] rings and [SiO<sub>3</sub>]<sub>∞</sub> chains, respectively, while the composition of CaSiO<sub>3</sub> glass is the same as that of melt ([SiO<sub>4</sub>], [SiO<sub>3</sub>]<sub>∞</sub>, [Si<sub>2</sub>O<sub>5</sub>]<sub>∞</sub>) [13]. Based on the structural characteristics, the preparation of  $\beta$ -CaSiO<sub>3</sub> glass–ceramics using CaSiO<sub>3</sub> glass is considered to be easier than that of  $\alpha$ -CaSiO<sub>3</sub> glass–ceramics.

Therefore, in this study, the microwave dielectric properties of  $\beta$ -CaSiO<sub>3</sub> glass–ceramics are investigated as a function of the holding time of the first step for homogeneous nucleation. Moreover, the microwave dielectric properties of  $\alpha$ -CaSiO<sub>3</sub> prepared using the solid-state reaction are investigated for comparison.

## 2. Materials and Methods

CaCO<sub>3</sub> (99.99%, Kojundo Chemical Laboratory Co., Ltd., Saitama, Japan) and SiO<sub>2</sub> (99.9%, Kojundo Chemical Laboratory Co., Ltd., Saitama, Japan) powders were used as raw materials and mixed with ZrO<sub>2</sub> balls for 24 h in ethanol and dried.  $\beta$ -CaSiO<sub>3</sub> ceramics were prepared using glass–ceramics method and  $\alpha$ -CaSiO<sub>3</sub> ceramics were prepared using the conventional solid-state reaction. For the  $\beta$ -CaSiO<sub>3</sub> glass–ceramics, the mixed powders were melted in a platinum crucible at 1590 °C for 3 h, and the melt was poured into distilled water. The glass frits were pulverized, sieved through 50 meshes, and re-milled for 24 h in ethanol. The dried glass powders were pressed with an isostatic pressure of 147 MPa to form pellets of 15 mm diameter and 7–8 mm thickness. The  $\beta$ -CaSiO<sub>3</sub> pellets were two-step heat-treated at 730 °C for 1–7 h, and then at 900 °C for 3 h. For  $\alpha$ -CaSiO<sub>3</sub>, the powders were calcined at 1200 °C for 2 h and re-milled in ethanol for 24 h. The dried powders were isostatically pressed with a pressure of 147 MPa to form pellets of 15 mm diameter and 7–8 mm thickness, and sintered at 1460–1500 °C for 3 h.

X-ray powder diffraction (XRD, Rigaku D/Max 2500 V/PC) was used to determine the crystalline phases and obtain the degree of crystallisation. The densities of the specimens were obtained using Archimedes' principle. Differential scanning calorimetry analysis (DSC) curves were obtained using a Simultaneous DSC (TA Instruments, SDT Q600, New Castle, DE, USA). Scanning electron microscopy (SEM, Hitachi SU-70/HORIBA) was performed to investigate the microstructure. The infrared absorption spectrum was obtained from 400 to 4000 cm<sup>-1</sup> using a Fourier infrared spectrometer (Thermo Scientific Nicolet iS50). The crystallinity of the specimens was investigated using Rietveld refinement [14,15]. The Rietveld refinements of the XRD patterns were performed using the FullProf program [16].  $\alpha$ -Al<sub>2</sub>O<sub>3</sub> (10 wt.%) was added to the specimens as an internal standard. Equation (1) was used to quantify the crystalline phases and degree of crystallisation of the specimens [15]. Equation (1) is as follows:

$$\alpha = (W_c/W_{std})(W_{std}/W) \quad (1)$$

where  $\alpha$ ,  $W$ ,  $W_c$ , and  $W_{std}$  are the degree of crystallisation, weight of the specimen, crystalline component, and internal standard, respectively. The dielectric constant ( $K$ ) and quality factor ( $Qf$ ) of the specimens were obtained from the microwave frequencies using the Hakki and Coleman method [17] with TE<sub>011</sub> mode in the range of 12–13 GHz. Network Analyzer (Agilent Technologies, E5071C, Santa Clara, CA, USA) was used for the measurement of dielectric properties ( $K$ ,  $Qf$ ,  $TCF$ ) of the sample at microwave frequencies. The  $TCF$  of the specimens was obtained using the cavity method [18].

### 3. Results and Discussion

#### 3.1. Phase Identification and Microwave Dielectric Properties of CaSiO<sub>3</sub> Ceramics

According to a previous study, it is difficult to obtain single-phase dense CaSiO<sub>3</sub> ceramics using the conventional solid-state reaction because of the narrow sintering windows of CaSiO<sub>3</sub> and its porous properties [19]. Since the structures of  $\beta$ -CaSiO<sub>3</sub> and CaSiO<sub>3</sub> glass are similar, single-phase  $\beta$ -CaSiO<sub>3</sub> can be obtained by the precipitation of the crystal phase from the glass using the glass–ceramic method. To improve the dielectric properties of the  $\beta$ -CaSiO<sub>3</sub> glass–ceramics by enhancing the degree of crystallisation, the specimens were heat-treated as a function of the nucleation holding time of the first-step heat treatment from 1 to 7 h. For comparison,  $\beta$ -CaSiO<sub>3</sub> sintered at 1100 °C for 3 h was prepared using the conventional solid-state reaction.

In Figure 1, differential scanning calorimetry analysis (DSC) was used to study the thermal behavior of CaSiO<sub>3</sub> glass powder. As a result, the starting exothermic temperature of crystallisation ( $T_c$ ) and strong exothermic peak temperature of crystallisation ( $T_p$ ) are observed. The exothermic reaction is the effect of crystallisation which accompanies the heat release. Therefore, the crystallisation temperature of CaSiO<sub>3</sub> glass could be identified by the strong exothermal peak from the DSC result. In this study, in order to meet the temperature condition of LTCC, 900 °C was selected as the crystallisation temperature, which is closest to the crystallisation temperature. However, DSC analysis did not show the nucleation temperature of CaSiO<sub>3</sub> glass. Therefore, the heat-treatment temperature of the nucleation stage in this study was set to 730 °C which is reported by Mohammadi et al. [12].

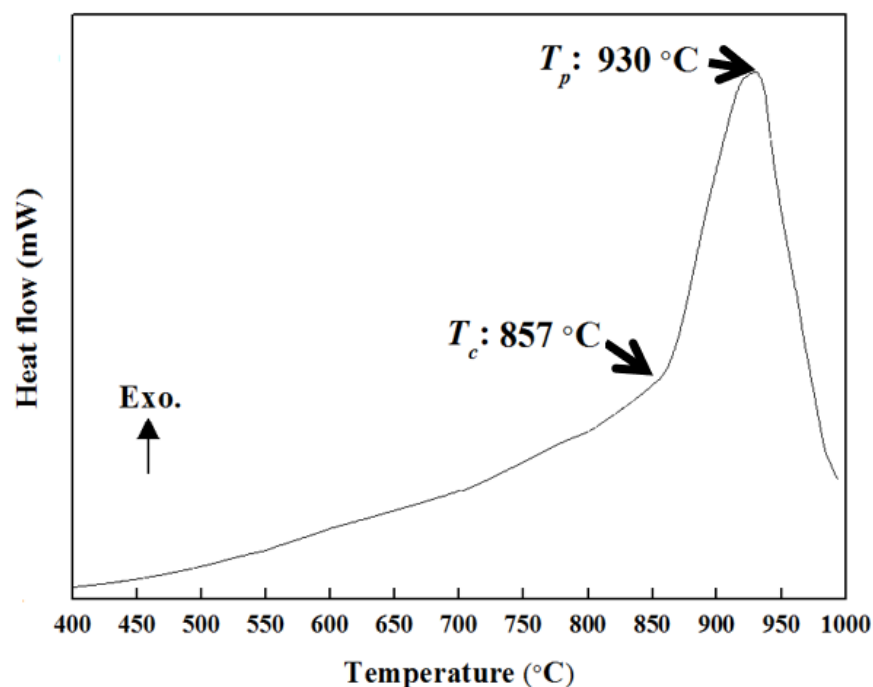
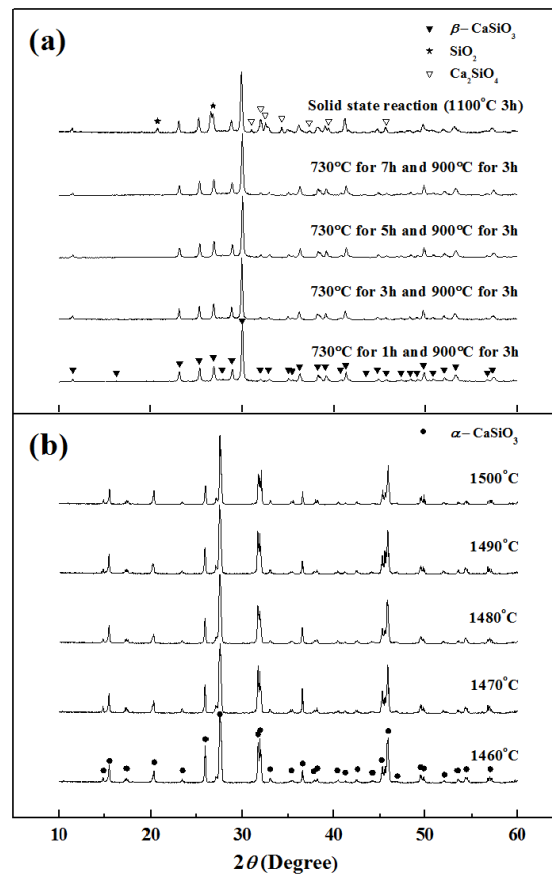


Figure 1. DSC curve of CaSiO<sub>3</sub> glass powder.

As shown in Figure 2a, the CaSiO<sub>3</sub> glass–ceramics were confirmed to be single-phase  $\beta$ -CaSiO<sub>3</sub> (JCPDS no. 01-075-1396) under all heat-treatment conditions, whereas CaSiO<sub>3</sub> prepared using the solid-state reaction exhibited Ca<sub>2</sub>SiO<sub>4</sub> (JCPDS no. 01-077-0388) and SiO<sub>2</sub> (JCPDS no. 03-065-0466) as secondary phases. Figure 2b shows the XRD patterns of  $\alpha$ -CaSiO<sub>3</sub> sintered at 1460–1500 °C for 3 h. All specimens exhibited single-phase  $\alpha$ -CaSiO<sub>3</sub> (JCPDS no. 01-074-0874), and no significant differences were observed with the change in the sintering temperature.



**Figure 2.** X-ray diffraction patterns of  $\text{CaSiO}_3$  ceramics. (a)  $\beta\text{-CaSiO}_3$  glass–ceramics heat-treated at 730 °C for 1–7 h and at 900 °C for 3 h, and  $\beta\text{-CaSiO}_3$  sintered at 1100 °C for 3 h, which is prepared using solid-state reaction. (b)  $\alpha\text{-CaSiO}_3$  sintered at 1460–1500 °C for 3 h, which is prepared using solid-state reaction.

Figure 3 shows the relative density and microwave dielectric properties of the  $\beta\text{-CaSiO}_3$  glass–ceramics and  $\alpha\text{-CaSiO}_3$ , respectively. As shown in Figure 3a, the relative density of the  $\beta\text{-CaSiO}_3$  glass–ceramics increases up to 97.38%, and then decreases to 96.17%. The slight decrease in the relative density can be attributed to the higher volume fraction of the  $\text{CaSiO}_3$  glass phase than that of the  $\beta\text{-CaSiO}_3$  crystal line phase owing to the smaller density of the  $\text{CaSiO}_3$  glass phase (2.89 g/cm<sup>3</sup>) than that of the  $\beta\text{-CaSiO}_3$  crystalline phase (2.92 g/cm<sup>3</sup>) [20,21]. It had been reported that the effect of porosity on the dielectric properties can be neglected because all specimens exhibit a relative density of above 96% [22]. Therefore, the dielectric constants of the  $\beta\text{-CaSiO}_3$  glass–ceramics exhibit a similar value of  $K = 6.57$  with the holding time during the first step heat treatment (nucleation) at 730 °C. The  $Q_f$  of the  $\beta\text{-CaSiO}_3$  glass–ceramics is higher than 46,000 GHz throughout the heat-treatment conditions. The  $\beta\text{-CaSiO}_3$  glass–ceramics heat-treated at 730 °C for 3 h and at 900 °C for 3 h exhibit the highest  $Q_f$  of 52,460 GHz, and then the  $Q_f$  decreases with the increase in holding time at 730 °C. However, as shown in Table 1,  $\beta\text{-CaSiO}_3$  prepared using the conventional solid-state reaction exhibits low density and dielectric properties. This indicates that the  $\beta\text{-CaSiO}_3$  glass–ceramics prepared using the two-step heat-treated glass–ceramics method exhibits a dense single phase and good dielectric properties. However, the effect of density is not sufficient to explain the tendency of the  $Q_f$  of  $\beta\text{-CaSiO}_3$  glass–ceramics because the relative density of that is over 96% for all heat-treatment conditions. Therefore, the degree of crystallisation of the glass–ceramics is studied, as mentioned in Section 3.2.

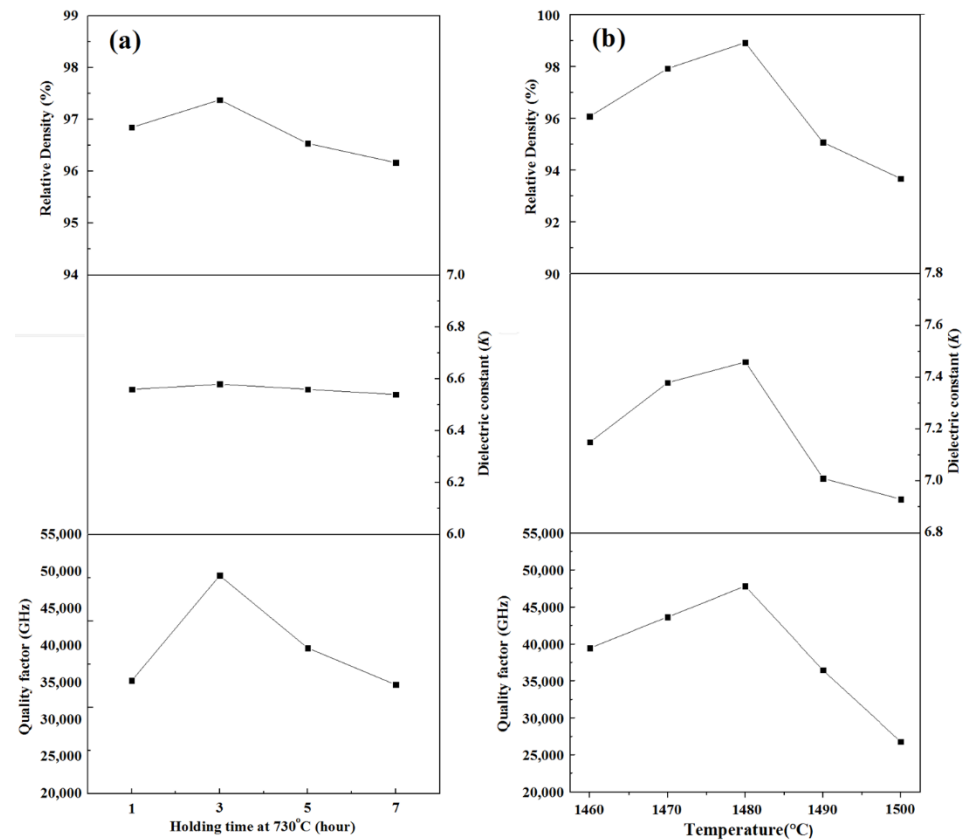


**Figure 3.** Relative Density, dielectric constant ( $K$ ), and quality factor ( $Q_f$ ) of (a)  $\beta$ -CaSiO<sub>3</sub> glass-ceramics heat-treated at 730 °C for 1–7 h and at 900 °C for 3 h, and of (b)  $\alpha$ -CaSiO<sub>3</sub> sintered at 1460–1500 °C for 3 h.

**Table 1.** Relative density and dielectric properties of  $\beta$ -CaSiO<sub>3</sub> prepared using (a) glass-ceramics method and heat-treated at 730 °C for 3 h and at 900 °C for 3 h, and that prepared using (b) solid-state reaction and sintered at 1100 °C for 3 h.

$\beta$ -CaSiO <sub>3</sub>	Relative Density [%]	$K$	$Q_f$ [GHz]
(a)	97.44	6.66	52640
(b)	58.07	4.45	2120

Figure 3b shows the relative density and microwave dielectric properties ( $K$ ,  $Q_f$ ) of  $\alpha$ -CaSiO<sub>3</sub> sintered at 1460–1500 °C for 3 h. As the sintering temperature increased to 1480 °C, the relative density and dielectric constant increased, reaching a maximum value of 98.93% and  $K = 7.45$ , respectively. However, for the specimens sintered at temperatures higher than 1480 °C, the relative density and dielectric constant of the specimens decreased. The  $Q_f$  of  $\alpha$ -CaSiO<sub>3</sub> also exhibited a maximum value of 47,870 GHz at a sintering temperature of 1480 °C, and decreased at higher sintering temperatures, which was similar to the relative density of the specimens. In general, the dielectric constant of the ceramics is affected by their density [23], which is in agreement with the results in this study.

Figures 4 and 5 show the SEM micrographs of  $\beta$ -CaSiO<sub>3</sub> glass-ceramics and  $\alpha$ -CaSiO<sub>3</sub>. As the holding time of the nucleation stage increased, the grain size increased up to 3 h (Figure 4b), and then the uniformity of microstructure deteriorated with further increase time of holding time. The inhomogeneity of the microstructure could be attributed to the newly formed nuclei with longer nucleation holding times. In the case of  $\alpha$ -CaSiO<sub>3</sub>, as the sintering temperature increased, the average grain size also increased and showed a homogeneous microstructure (Figure 5c) at 1480 °C for 3 h. However, as the sintering temperature increased above 1490 °C, pores and deterioration in the uniformity of the

microstructure were observed (Figure 5d,e). The change in the microstructure with increasing sintering temperature could be attributed to the formation of excess liquid phase during the sintering, as confirmed by a phase diagram of the CaO–SiO<sub>2</sub> system [24]. This result is consistent with the relative density of  $\alpha$ -CaSiO<sub>3</sub>, which indicates that the dielectric properties of  $\alpha$ -CaSiO<sub>3</sub> are affected by the density and microstructure. Since  $\beta$ -CaSiO<sub>3</sub> was prepared by the glass–ceramics method, the heat-treatment temperature was much lower than that of  $\alpha$ -CaSiO<sub>3</sub>. Therefore, the grain size of  $\beta$ -CaSiO<sub>3</sub> was smaller than that of  $\alpha$ -CaSiO<sub>3</sub>. However,  $\beta$ -CaSiO<sub>3</sub> showed higher  $Q_f$  than  $\alpha$ -CaSiO<sub>3</sub>, which indicates the  $Q_f$  of  $\beta$ -CaSiO<sub>3</sub> and  $\alpha$ -CaSiO<sub>3</sub> was significantly influenced by other factors.

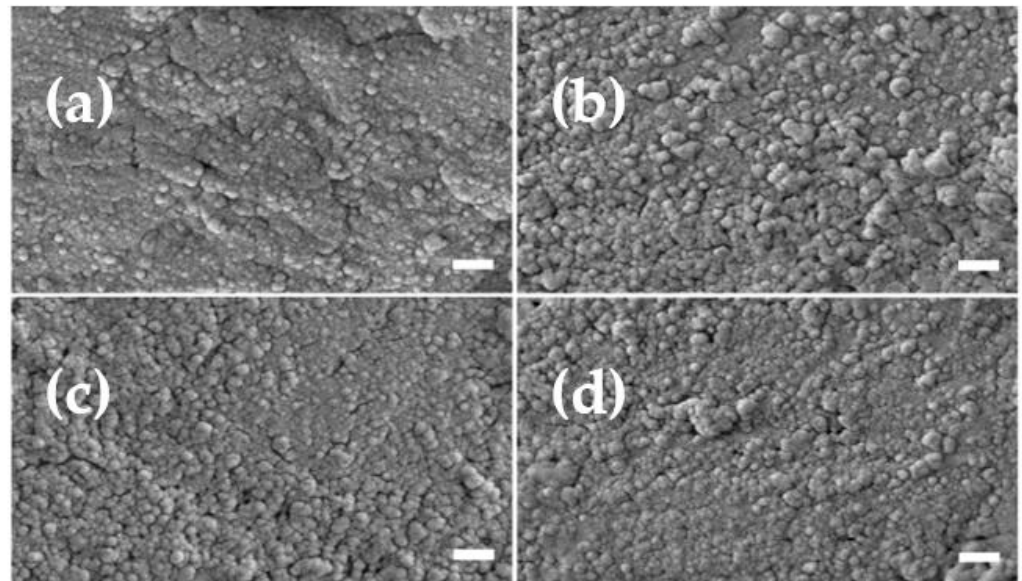


**Figure 4.** SEM micrographs of  $\beta$ -CaSiO<sub>3</sub> glass-ceramics specimens heat-treated at 730 °C for x h and 900 °C for 3 h (a) x = 1 (b) x = 3 (c) x = 5 (d) x = 7 (bar = 0.5  $\mu$ m).

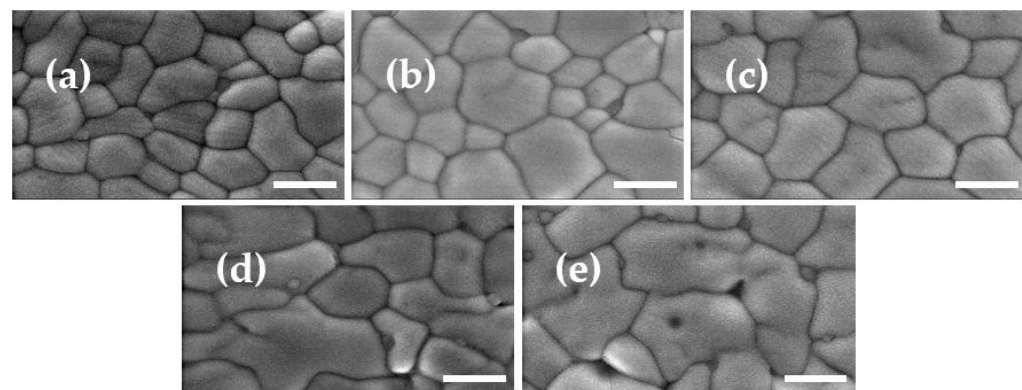


**Figure 5.** SEM micrographs  $\alpha$ -CaSiO<sub>3</sub> specimens sintered at (a) 1460 °C (b) 1470 °C (c) 1480 °C (d) 1490 °C and (e) 1500 °C for 3 h (bar = 0.5  $\mu$ m).

### 3.2. Degree of Crystallisation and Structural Analysis of $\beta$ -CaSiO<sub>3</sub> and $\alpha$ -CaSiO<sub>3</sub>

As described in Section 3.1, the relative density is not sufficient to explain the dielectric properties of the  $\beta$ -CaSiO<sub>3</sub> glass–ceramics. Therefore, the degree of crystallisation of  $\alpha$ -CaSiO<sub>3</sub> is investigated because the high sintering temperature of  $\alpha$ -CaSiO<sub>3</sub> can be associated with the liquid phase. According to the phase diagram of the CaO–SiO<sub>2</sub> system [24], the co-existence region with the liquid phase exists on both sides of the CaSiO<sub>3</sub> composition line at temperatures above 1436 °C. In addition, as the sintering temperature of  $\alpha$ -CaSiO<sub>3</sub> increases, the proportion of the liquid phase increases according to the lever rule. Therefore, the degree of crystallisation of  $\alpha$ -CaSiO<sub>3</sub> is also investigated.

The Rietveld quantitative analyses of the  $\beta$ -CaSiO<sub>3</sub> glass–ceramics prepared under various heat-treatment conditions and that of  $\alpha$ -CaSiO<sub>3</sub> sintered at 1480 °C for 3 h were performed based on the XRD data. Toby et al. [25] reported that the most crucial method to evaluate the quality of Rietveld refinement is to graphically compare the observed and calculated patterns. Therefore, the validity of the Rietveld analysis in this study was supported by the Rietveld refinement results, and the Rietveld refinement parameters (goodness of fit,  $\chi^2$ ), are shown in Figure 6 and Table 2. Furthermore, the weight fraction (%) of the specimens and internal standard, and the results of the degree of crystallisation of the  $\beta$ -CaSiO<sub>3</sub> glass–ceramics are shown in Table 2. It can be confirmed that the results were consistent with low  $\chi^2$ , indicating that they were reliable.

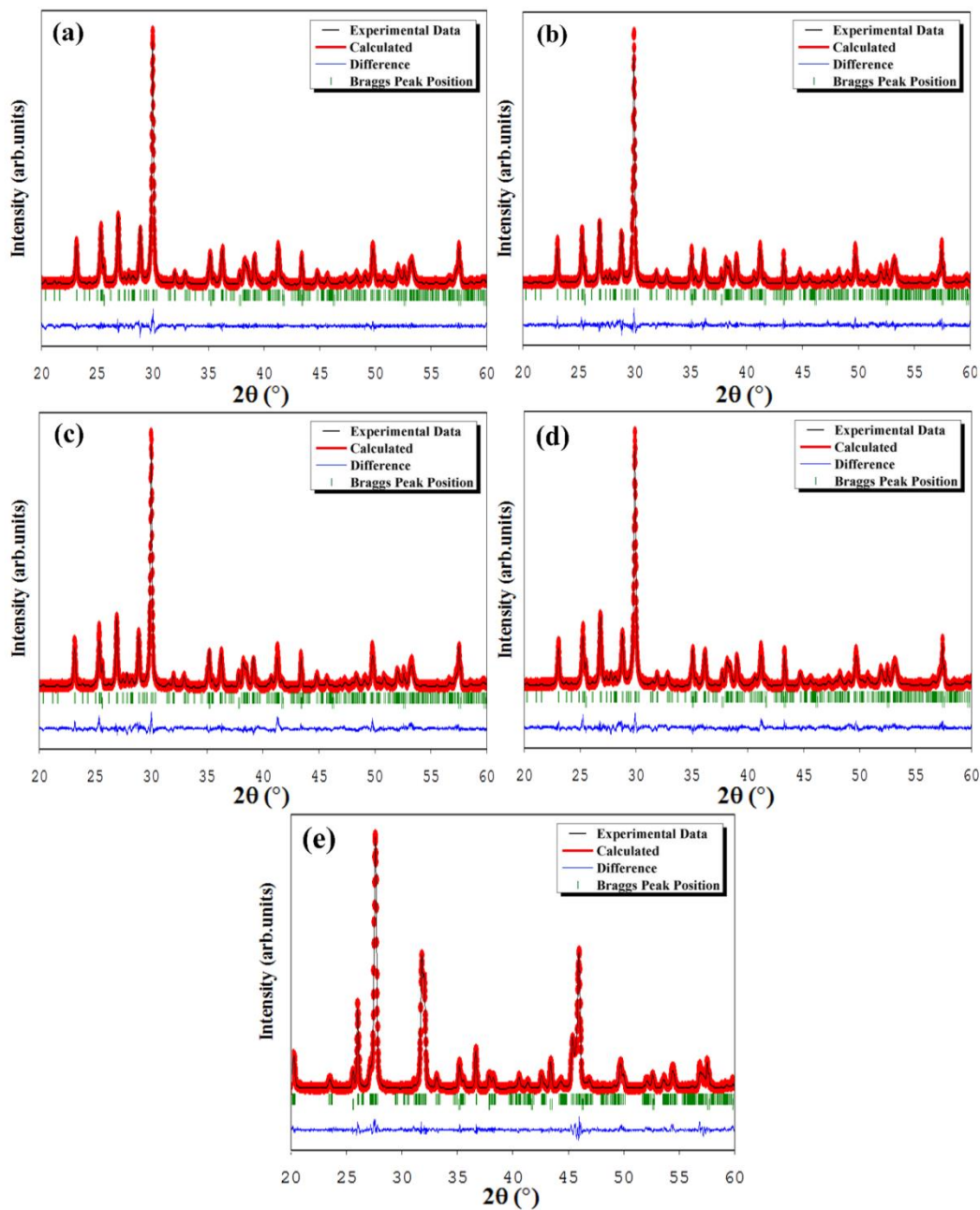


**Figure 6.** Rietveld-refined X-ray diffraction patterns of  $\beta$ -CaSiO<sub>3</sub> glass–ceramics heat-treated at 730 °C for x h and 900 °C for 3 h, where x = (a) 1, (b) 3, (c) 5, and (d) 7, and of (e)  $\alpha$ -CaSiO<sub>3</sub> sintered at 1480 °C for 3 h.

**Table 2.** Rietveld quantitative analysis of  $\beta$ -CaSiO<sub>3</sub> glass–ceramics heat-treated at 730 °C for 1–7 h and 900 °C for 3 h and  $\alpha$ -CaSiO<sub>3</sub> sintered at 1480 °C for 3 h.

Phase	$\beta$				$\alpha$
Process	Glass-Ceramics				Solid State Reaction
Heat-treatment conditions	730 °C/1 h And 900 °C/3 h	730 °C/3 h And 900 °C/3 h	730 °C/5 h And 900 °C/3 h	730 °C/7 h And 900 °C/3 h	1480 °C/3 h
CaSiO <sub>3</sub> (wt.%)	87.03	87.71	87.39	86.94	88.56
Al <sub>2</sub> O <sub>3</sub> (wt.%)	12.97	12.29	12.61	13.06	11.44
Degree of crystallisation (%)	74.56	79.30	77.00	73.67	86.01
GoF	2.6	2.5	3.1	2.9	3.1
R <sub>wp</sub>	10.9	10.5	11.4	11.5	10.8
RF factor (CaSiO <sub>3</sub> )	4.31	3.98	3.87	4.22	3.72
RF factor (Al <sub>2</sub> O <sub>3</sub> )	2.06	1.99	2.60	2.21	2.37

The degree of crystallisation of  $\beta$ -CaSiO<sub>3</sub> is graphically shown in Figure 7. As the holding time of the first step (nucleation step) increased, the degree of crystallisation increased and reached a maximum value of 79.3% under the heat-treatment condition of 730 °C for 3 h and of 900 °C for 3 h. However, as the holding time of the first step increased over 3 h, the degree of crystallisation decreased again. According to Ramesh et al. [6], the degree of crystallisation of glass decreases with an increase in holding time owing to the instability of critical-sized nuclei, when they are heat-treated at the nucleation step for a long time. Therefore, in this study,  $\beta$ -CaSiO<sub>3</sub> heat-treated at 730 °C for 5 h, and/or 7 h, showed a decrease in the degree of crystallisation and the degradation of the dielectric properties of the specimens. The degree of crystallisation showed a similar tendency to the  $Q_f$ , which indicated that the  $Q_f$  of the  $\beta$ -CaSiO<sub>3</sub> glass–ceramics was significantly influenced by the degree of crystallisation of the specimens. In addition, the tendency of relative density is dependent on the relative ratio of crystalline phase to glass phase, and the density of  $\beta$ -CaSiO<sub>3</sub> crystalline (2.92 g/cm<sup>3</sup>) is higher than that of CaSiO<sub>3</sub> glass (2.89 g/cm<sup>3</sup>) [20,21]. The relative density of the specimens increased with the increase of the crystalline phase, which could be evaluated by the degree of crystallisation. Therefore, the change of the relative density could be attributed to the effect of the degree of crystallisation (Figure 3 and Table 2).

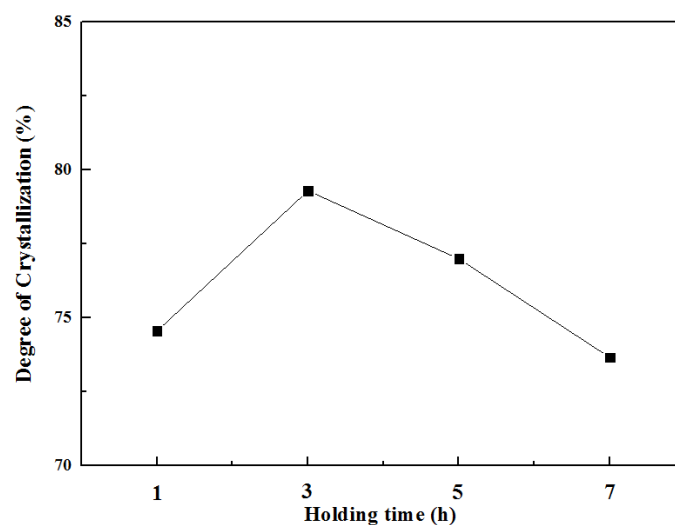
**Figure 7.** Degree of crystallisation of  $\beta$ -CaSiO<sub>3</sub> glass–ceramics heat-treated at 730 °C for 1–7 h and at 900 °C for 3 h.

Table 2 shows the degree of crystallisation for  $\beta$ -CaSiO<sub>3</sub> and  $\alpha$ -CaSiO<sub>3</sub> prepared under various heat-treatment conditions. As shown in Table 2,  $\alpha$ -CaSiO<sub>3</sub> showed a higher degree of crystallisation than  $\beta$ -CaSiO<sub>3</sub>. However,  $\beta$ -CaSiO<sub>3</sub> showed more improved dielectric properties than  $\alpha$ -CaSiO<sub>3</sub>, despite the lower degree of crystallisation and relative density, as shown in Figure 3 and Table 2.

The  $Q_f$  of the specimens depends on extrinsic factors, such as relative density and microstructure, and on intrinsic factors, such as crystal structure and bond characteristics [26]. As described in Section 1 (Introduction),  $\beta$ -CaSiO<sub>3</sub> has a SiO<sub>4</sub> tetrahedral chain structure with three symmetrically non-equivalent Ca sites, seven Ca–O bonds, three Si sites and four Si–O bonds [8].  $\alpha$ -CaSiO<sub>3</sub> has a three-membered SiO<sub>4</sub> tetrahedral ring structure with five symmetrically non-equivalent Ca sites, eight Ca–O bonds, three Si sites and four Si–O bonds [9]. To investigate the effect of the crystal structure and bond characteristics on the microwave dielectric properties of  $\beta$ -CaSiO<sub>3</sub> and  $\alpha$ -CaSiO<sub>3</sub> phases, the bond strength of each phase was calculated from the bond lengths between cation and oxygen. Equation (2) [27] is as follows:

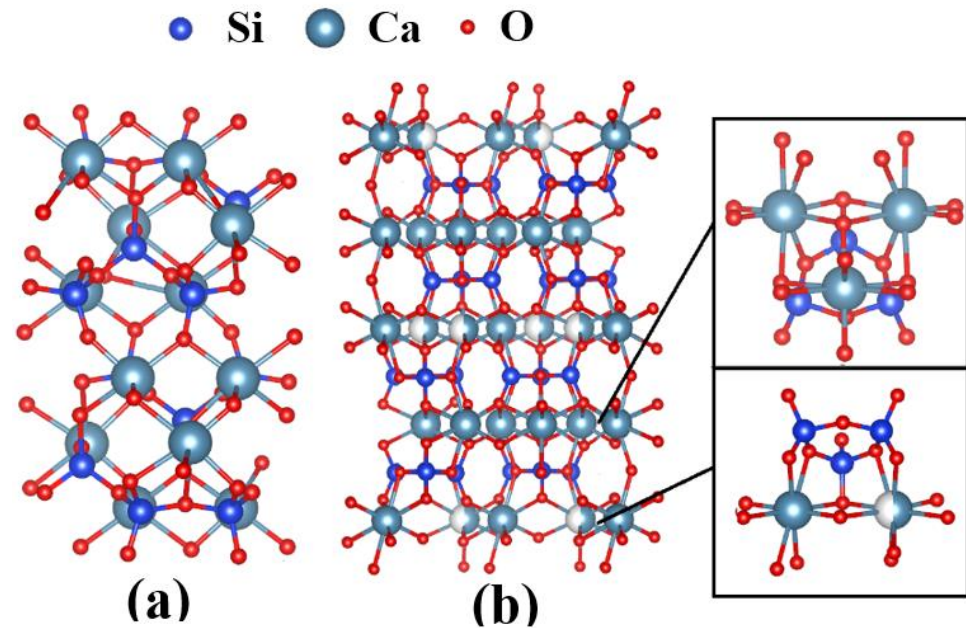
$$\langle s \rangle = s_0 \left( \frac{R}{R_0} \right)^{-N} \quad (2)$$

where  $s$ ,  $s_0$ ,  $R$ ,  $R_0$ , and  $N$  are the calculated bond strength, ideal bond strength, bond length obtained by XRD Rietveld refinement, ideal bond length, and constant, respectively, for each cation–anion pair. The ideal bond strength,  $s_0$ , and ideal bond length,  $R_0$ , are constants value-corrected for oxygen coordination for each M–O pair [27]. Each term and calculated bond strength ( $\langle S_{\text{Ca-O}} \rangle$ ,  $\langle S_{\text{Si-O}} \rangle$ ) by average bond length,  $R_{\text{avg}}$ , are shown in Table 3. The bond lengths of the Ca–O and Si–O bonds for each symmetrically non-equivalent site were obtained by crystal structure (Figure 8) from XRD Rietveld refinement and summarized in Table 4. Figure 8a shows the SiO<sub>4</sub> chain structure of  $\beta$ -CaSiO<sub>3</sub> and three Ca sites where seven Ca–O bonds could be observed. The three-membered SiO<sub>4</sub> ring structure of  $\alpha$ -CaSiO<sub>3</sub> and five Ca site with eight Ca–O bonds could also be observed in Figure 8b. In the case of the bond strength of Si–O  $\langle S_{\text{Si-O}} \rangle$ , it was confirmed that  $\alpha$ -CaSiO<sub>3</sub> showed a slightly higher bond strength than that of  $\beta$ -CaSiO<sub>3</sub>. In the case of the bond strength of Ca–O  $\langle S_{\text{Ca-O}} \rangle$ ,  $\beta$ -CaSiO<sub>3</sub> exhibited a higher bond strength than that of  $\alpha$ -CaSiO<sub>3</sub>, and their difference was greater than that of  $\langle S_{\text{Si-O}} \rangle$ . This result indicates that the bond strength of Ca–O may significantly influence the dielectric properties of CaSiO<sub>3</sub>.

Figure 9 shows the infrared absorption spectrum of  $\beta$ -CaSiO<sub>3</sub> and  $\alpha$ -CaSiO<sub>3</sub> ranging from 400 to 4000 cm<sup>−1</sup>. In Figure 9a, the presence of  $\beta$ -CaSiO<sub>3</sub> is confirmed by the symmetric stretching vibration mode of the Si–O–Si bridges within the range of 563–680 cm<sup>−1</sup>, and asymmetric, symmetric stretching vibration modes of Si–O–Si and O–Si–O within the range of 897–1092 cm<sup>−1</sup>. The absorption band at 452 cm<sup>−1</sup> represents the bending of the Si–O non-bridge mode [28,29]. In Figure 9b, the presence of  $\alpha$ -CaSiO<sub>3</sub> is confirmed by the bands at 441 cm<sup>−1</sup>, 562 cm<sup>−1</sup>, 713 cm<sup>−1</sup>, 921 cm<sup>−1</sup>, 936 cm<sup>−1</sup>, 982 cm<sup>−1</sup>, 1071–1092 cm<sup>−1</sup> which were related to the Si–O bond [30]. The stretching vibration of Si–O at 714 cm<sup>−1</sup> indicates the presence of a three-membered ring and the bands within 922–1092 cm<sup>−1</sup> indicate the stretching vibration of an Si–O bridge and non-bridge [31]. There are no other vibration modes above 1200 cm<sup>−1</sup> for both spectra of  $\beta$ -CaSiO<sub>3</sub> and  $\alpha$ -CaSiO<sub>3</sub>. As the vibration mode associated with Ca<sup>2+</sup> did not appear, it is considered to be located in the far-infrared region, which is outside the measuring range of the equipment. Therefore, it can be concluded that the vibration mode of Ca–O is located at the lowest frequency. Because the vibration mode with the lowest frequency significantly influences the dielectric loss ( $\tan\delta$ ),  $\beta$ -CaSiO<sub>3</sub> exhibits a higher  $Q_f$  ( $Q_f = 1/\tan\delta$ ) even with a lower degree of crystallisation than that of  $\alpha$ -CaSiO<sub>3</sub> (Table 2). These results are in agreement with the results of Bian J. et al. [32], in which the lowest frequency vibration mode significantly affects the microwave dielectric loss, and the vibration mode associated with Ca<sup>2+</sup> is located in the far infrared range for Ca<sub>2</sub>P<sub>2</sub>O<sub>7</sub> systems. The temperature coefficient of resonant frequency (TCF) of the  $\beta$ -CaSiO<sub>3</sub> glass–ceramics is −36.22 ppm/°C under all heat-treatment conditions.

**Table 3.** Average bond length, constant and calculated bond strength of Si–O and Ca–O bonds of  $\beta$ -CaSiO<sub>3</sub> and  $\alpha$ -CaSiO<sub>3</sub>.

CaSiO <sub>3</sub>	Ca–O Bond					Si–O Bond				
	R <sub>avg</sub>	R <sub>0</sub>	s <sub>0</sub>	N	<S <sub>Ca-O</sub> >	R <sub>avg</sub>	R <sub>0</sub>	s <sub>0</sub>	N	<S <sub>Si-O</sub> >
$\beta$	2.405	2.437	0.25	5.5	0.270	1.654	1.605	1.0	4.0	0.893
$\alpha$	2.565	2.437	0.25	5.5	0.193	1.629	1.605	1.0	4.0	0.942

**Figure 8.** Crystal structure of (a)  $\beta$ -CaSiO<sub>3</sub> and (b)  $\alpha$ -CaSiO<sub>3</sub>.**Table 4.** Bond length of Si–O and Ca–O bonds for each symmetrically non-equivalent site (<Ca–O><sub>x</sub>) of  $\beta$ -CaSiO<sub>3</sub> and  $\alpha$ -CaSiO<sub>3</sub>.

CaSiO <sub>3</sub>	<Ca–O> <sub>1</sub>	<Ca–O> <sub>2</sub>	<Ca–O> <sub>3</sub>	<Ca–O> <sub>4</sub>	<Ca–O> <sub>5</sub>	<Si–O> <sub>1</sub>	<Si–O> <sub>2</sub>	<Si–O> <sub>3</sub>
$\beta$	2.323	2.31	2.37			1.64248	1.62	1.734
	2.05	2.38	2.27			1.57	1.65065	1.66443
	2.32	2.368	2.472			1.6475	1.52	1.66245
	2.755	2.27	2.2			1.75	1.6014	1.79
	2.7	2.16	2.49					
	2.54	2.46	2.51					
	2.55	2.59	2.42					
$\alpha$	2.3106	2.6854	2.6367	2.3422	2.3351	1.66384	1.6619	1.5929
	2.5742	2.5685	2.6326	2.5811	2.5992	1.66256	1.5844	1.6627
	2.5984	2.5609	2.5779	2.5885	2.5882	1.5939	1.5839	1.6621
	2.6796	2.6489	2.2821	2.6682	2.6626	1.5835	1.6611	1.6389
	2.3106	2.5609	2.5951	2.5811	2.6626			
	2.5742	2.6854	2.2811	2.3422	2.5882			
	2.6796	2.5685	2.5971	2.6682	2.3351			
	2.5984	2.6489	2.5666	2.5885	2.5992			

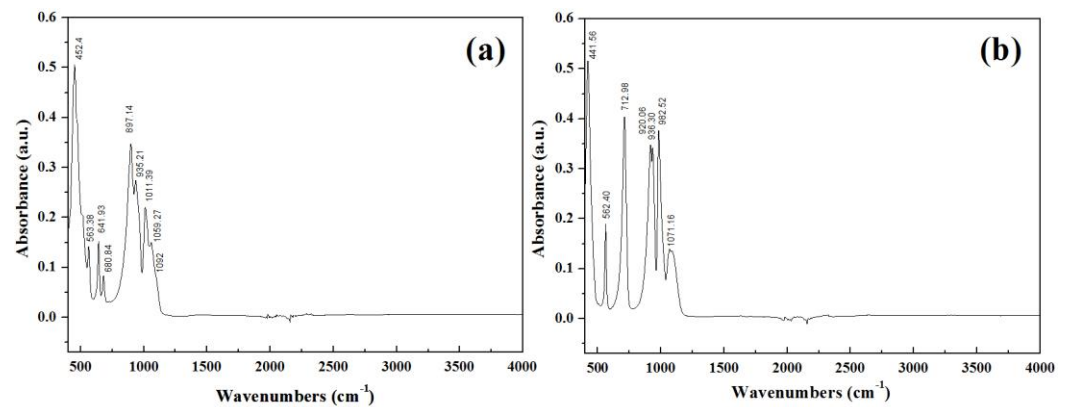


**Figure 9.** Fourier transform infrared-Attenuated Total Reflectance (FTIR-ATR) spectra of (a)  $\beta$ -CaSiO<sub>3</sub> glass-ceramics heat-treated at 730 °C for 3 h and at 900 °C for 3 h (b)  $\alpha$ -CaSiO<sub>3</sub> ceramics sintered at 1480 °C for 3 h.

#### 4. Conclusions

$\beta$ -CaSiO<sub>3</sub> and  $\alpha$ -CaSiO<sub>3</sub> were prepared using glass-ceramics and solid-state reaction methods, respectively.  $\beta$ -CaSiO<sub>3</sub> with a single phase was obtained using the glass-ceramics method with two-step heat treatment. The dielectric properties of the  $\beta$ -CaSiO<sub>3</sub> glass-ceramics were not dependent on the density of the specimens, and a similar dielectric constant ( $K$ ) was obtained for the  $\beta$ -CaSiO<sub>3</sub> glass-ceramics with a change in the holding time of 730 °C as the first step of heat treatment. The  $Q_f$ s of the specimens were constant ( $K$ ) were obtained for the  $\beta$ -CaSiO<sub>3</sub> glass-ceramics with a change in the holding time of 730 °C as the first step of heat treatment. The  $Q_f$ s of the specimens were strongly dependent on the degree of crystallisation, which was affected by the holding time of the first step of the heat treatment. The  $\beta$ -CaSiO<sub>3</sub> glass-ceramics heat treated at 730 °C for 3 h and at 900 °C for 3 h exhibited a degree of crystallisation of 79.3%,  $K$  of 6.57, and  $Q_f$  of 52,640 GHz. The dielectric properties of the  $\alpha$ -CaSiO<sub>3</sub> specimens were associated with the density and microstructure, and the specimens sintered at 1480 °C for 3 h exhibited the dielectric properties of  $K = 7.45$  and  $Q_f = 47,870$  GHz.

The  $Q_f$  difference between  $\beta$ -CaSiO<sub>3</sub> and  $\alpha$ -CaSiO<sub>3</sub> was investigated by the bond characteristics using the Rietveld refinement of the XRD patterns. The results showed that the Ca–O bond strength of  $\beta$ -CaSiO<sub>3</sub> was higher than that of  $\alpha$ -CaSiO<sub>3</sub>, and the  $Q_f$  was significantly dependent on the Ca–O bond strength, which was confirmed using FT-IR analysis. The  $\beta$ -CaSiO<sub>3</sub> glass-ceramics exhibited good dielectric properties of  $K = 6.57$ ,  $Q_f = 52,640$  GHz, and  $TCF = -36.22$  ppm/°C at low heat-treatment temperatures of 730 °C for 3 h and of 900 °C for 3 h. Therefore, the  $\beta$ -CaSiO<sub>3</sub> glass-ceramics might be promising candidates for LTCC materials.

**Author Contributions:** E.-S.K. and J.-S.B. designed the experiments. J.-S.B. and N.-B.J. performed the experiments and analysed the specimens. J.-S.B. analysed and explained the dependence of microwave dielectric properties on bond characteristics of the specimens. All the authors discussed the data and wrote the manuscript. All authors have read and agreed to the published version of the manuscript.

**Funding:** This research was supported by the National Research Foundation of Korea(NRF) grant funded by the Korea government(MSIT) (No. 2019R1F1A1062810).

**Institutional Review Board Statement:** Not applicable.

**Informed Consent Statement:** Not applicable.

**Data Availability Statement:** Not applicable.

**Acknowledgments:** A part of this work was also supported by Kyonggi University Graduate Research Assistantship 2021.

**Conflicts of Interest:** The authors declare no conflict of interest.

## References

1. Sebastian, M.T.; Jantunen, H. High Temperature Cofired Ceramic (HTCC), Low Temperature Cofired Ceramic (LTCC), and Ultralow Temperature Cofired Ceramic (ULTCC) Materials. *Microw. Mater. Appl.* **2017**, *2*, 355–425.
2. Uchikoba, F.; Nakajima, S.; ITO, T. Fabrication of Multilayer Capacitors with Silver Internal Electrodes and Alumina-Glass Composite Materials. *J. Ceram. Soc. Jpn.* **1995**, *103*, 969–973. [[CrossRef](#)]
3. Chen, G.; Liu, X. Fabrication, Characterization and Sintering of Glass-Ceramics for low-Temperature Co-Fired Ceramic SUBSTRATES. *J. Mater. Sci. Mater. Electron.* **2004**, *15*, 595–600. [[CrossRef](#)]
4. Sebastian, M.T.; Jantunen, H. Low Loss Dielectric Materials for LTCC Applications: A Review. *Int. Mater. Rev.* **2008**, *53*, 57–90. [[CrossRef](#)]
5. Oxtoby, D.W. Homogeneous Nucleation: Theory and Experiment. *J. Phys. Condens. Matter* **1992**, *4*, 7627–7650. [[CrossRef](#)]
6. Ramesh, R.; Nestor, E.; Pomeroy, M.J.; Hampshire, S. Classical and Differential Thermal Analysis Studies of the Glass-Ceramic Transformation in a YSiAlON Glass. *J. Am. Ceram. Soc.* **2005**, *81*, 1285–1297. [[CrossRef](#)]
7. Lin, K.; Chang, J.; Zeng, Y.; Qian, W. Preparation of Macroporous Calcium Silicate Ceramics. *Mater. Lett.* **2004**, *58*, 2109–2113. [[CrossRef](#)]
8. Deer, W.A.; Howie, R.A.; Zussman, J. *Single-Chain Silicates. Rock-Forming Minerals*, 2nd ed.; Geological Society: London, UK, 1997; Volume 2A, p. 547.
9. Yang, H.; Prewitt, C.T. On the Crystal Structure of Pseudowollastonite(CaSiO<sub>3</sub>). *Am. Mineral.* **1999**, *84*, 929–932. [[CrossRef](#)]
10. Li, D.; Wang, H.; He, Z.; Xiao, Z.; Lei, R.; Xu, S. Effect of CuO Addition on the Sintering Temperature and Microwave Dielectric Properties of CaSiO<sub>3</sub>-Al<sub>2</sub>O<sub>3</sub> Ceramics. *Prog. Nat. Sci.* **2014**, *24*, 274–279. [[CrossRef](#)]
11. Isao, K.; Itaru, S.; Hitoshi, O. Microwave Dielectric Properties of (Ca<sub>1-x</sub>Sr<sub>x</sub>)SiO<sub>3</sub> Ring Silicate Solid Solutions. *Jpn. J. Appl. Phys.* **2009**, *48*, 09KE02.
12. Mohammadi, M.; Alizadeh, P.; Atlasbaf, Z. Effect of Frit Size on Sintering, Crystallization and Electrical Properties of Wollastonite Glass-Ceramics. *J. Non-Cryst. Solids* **2011**, *357*, 150–156. [[CrossRef](#)]
13. Voron'ko, Y.K.; Sobol', A.A.; Ushakov, S.N.; Jiang, G.; You, J. Phase Transformations and Melt Structure of Calcium Metasilicate. *Inorg. Mater.* **2002**, *38*, 825–830. [[CrossRef](#)]
14. Barbieri, L.; Bondioli, F.; Lancellotti, I.; Leonelli, C.; Montorsi, M.; Ferrari, A.M.; Miselli, P. The Anorthite-Diopside System: Structural and Devitrification Study. Part II: Crystallinity Analysis by the Rietveld-RIR Method. *J. Am. Ceram. Soc.* **2005**, *88*, 3131–3136. [[CrossRef](#)]
15. Yasukawa, K.; Terashi, Y.; Nakayama, A. Crystallinity Analysis of Glass-Ceramics by the Rietveld Method. *J. Am. Ceram. Soc.* **2005**, *81*, 2978–2982. [[CrossRef](#)]
16. Roisnel, T.; Rodríguez-carvajal, J. WinPLOTR: A Windows Tool for Powder Diffraction Pattern Analysis. *Mater. Sci. Forum* **2001**, *378–381*, 118–123. [[CrossRef](#)]
17. Hakki, B.W.; Coleman, P.D. A Dielectric Resonator Method of Measuring inductive Capacities in the Millimeter Range. *IRE Trans. Microw. Theory Technol.* **1960**, *8*, 402–410. [[CrossRef](#)]
18. Nishikawa, T.; Wakino, K.; Tamura, H.; Tanaka, H.; Ishikawa, Y. Precise Measurement Method for Temperature Coefficient of Microwave Dielectric Resonator Material. *IEEE MTT-S Int. Microw. Symp. Dig.* **1987**, *1*, 277–280.
19. Sreekanth, C.R.P.; Nagabhushana, B.M.; Chandrappa, G.T.; Ramesh, K.P.; Rao, J.L. Solution Combustion Derived NANOCRYSTALLINE Macroporous Wollastonite Ceramics. *Mater. Chem. Phys.* **2006**, *95*, 169–175. [[CrossRef](#)]
20. Taniguchi, T.; Okuno, M.; Matsumoto, T. X-ray Diffraction and EXAFS Studies of Silicate Glasses Containing Mg, Ca and Ba Atoms. *J. Non-Cryst. Solids* **1997**, *211*, 56–63. [[CrossRef](#)]
21. Hesse, K.-F. Refinement of the Crystal Structure of Wollastonite-2M (Parawollastonite). *Z. Kristallogr. Cryst. Mater.* **1984**, *168*, 93–98. [[CrossRef](#)]
22. Iddles, D.M.; Bell, A.J.; Moulson, A.J. Relationships between Dopants, Microstructure and the Microwave Dielectric Properties of ZrO<sub>2</sub>-TiO<sub>2</sub>-SnO<sub>2</sub> Ceramics. *J. Mater. Sci.* **1992**, *27*, 6303–6310. [[CrossRef](#)]
23. Penn, S.J.; Alford, N.M.; Templeton, A.; Wang, X.; Xu, M.; Reece, M.; Schrapel, K. Effect of Porosity and Grain Size on the Microwave Dielectric Properties of Sintered Alumina. *J. Am. Ceram. Soc.* **2005**, *80*, 1885–1888. [[CrossRef](#)]
24. Hewlett, P.; Liska, M. *Lea's Chemistry of Cement and Concrete*; Butterworth-Heinemann: Oxford, UK, 2019.
25. Toby, B.H. R Factors in Rietveld Analysis: How Good Is Good Enough? *Powder Diffr.* **2006**, *21*, 67–70. [[CrossRef](#)]
26. Singh, S.K.; Murthy, V.R.K. Crystal Structure, Raman Spectroscopy and Microwave Dielectric Properties of Layered-Perovskite BaA<sub>2</sub>Ti<sub>3</sub>O<sub>10</sub> (A = La, Nd and Sm) Compounds. *Mater. Chem. Phys.* **2015**, *160*, 187–193. [[CrossRef](#)]
27. Brown, I.D.; Shannon, R.D. Empirical Bond-Strength–Bond-Length Curves for Oxides. *Acta Cryst. A* **1973**, *29*, 266–282. [[CrossRef](#)]
28. Zulumyan, N.; Mirgorodski, A.; Isahakyan, A.; Beglaryan, H.; Gabrielyan, A.; Terzyan, A. A Low-Temperature Method of the β–Wollastonite Synthesis. *J. Therm. Anal. Calorim.* **2015**, *122*, 97–104. [[CrossRef](#)]
29. Zhao, C.; Wang, G.; Li, S.; Ai, X.; Wang, Z.; Zhai, Y. Reaction Pathway Led by Silicate Structure Transformation on Decomposition of CaSiO<sub>3</sub> in Alkali Fusion Process Using NaOH. *Trans. Nonferrous Met. Soc. China* **2015**, *25*, 3827–3833. [[CrossRef](#)]
30. Bobkova, N.M.; Tizhovka, Z.S.; Tizhovka, V.V. A Spectroscopic Study of the Structure of Glasses in the CaO-SiO<sub>2</sub> System. *J. Appl. Spectrosc.* **1979**, *30*, 99–102. [[CrossRef](#)]

- 
31. Paluszkiewicz, C.; Blazewicz, M.; Podporska, J.; Gumula, T. Nucleation of Hydroxyapatite Layer on Wollastonite Material Surface: FTIR Studies. *Vib. Spectrosc.* **2008**, *48*, 263–268. [[CrossRef](#)]
  32. Bian, J.; Kim, D.-W.; Hong, K.S. Microwave Dielectric Properties of  $\text{Ca}_2\text{P}_2\text{O}_7$ . *J. Eur. Ceram. Soc.* **2003**, *23*, 2589–2592. [[CrossRef](#)]